



Concentrated LiODFB Electrolyte for Lithium Metal Batteries

Juan Yu¹, Na Gao¹, Jiaxin Peng¹, Nani Ma¹, Xiaoyan Liu², Chao Shen², Keyu Xie² and Zhao Fang^{1*}

¹ School of Metallurgical Engineering, Xi'an University of Architecture and Technology, Xi'an, China, ² State Key Laboratory of Solidification Processing, Center for Nano Energy Materials, School of Materials Science and Engineering, Northwestern Polytechnical University and Shaanxi Joint Laboratory of Graphene (NPU), Xi'an, China

Nowadays, lithium (Li) metal batteries arouse widespread concerns due to its ultrahigh specific capacity (3,860 mAh g⁻¹). However, the growth of Li dendrites has always limited their industrial development. In this paper, the use of concentrated electrolyte with lithium difluoro(oxalate)borate (LiODFB) salt in 1, 2-dimethoxyethane (DME) enables the good cycling of a Li metal anode at high Coulombic efficiency (up to 98.1%) without dendrite growth. Furthermore, a Li/Li cell can be cycled at 1 mA cm⁻² for over 3,000 h. Besides, compared to conventional LiPF₆-carbonate electrolyte, Li/LiFePO₄ cells with 4 M LiODFB-DME exhibit superior electrochemical performances, especially at high temperature (65°C). These outstanding performances can be certified to the increased availability of Li⁺ concentration and the merits of LiODFB salt. We believe that the concentrated LiODFB electrolyte is help to enable practical applications for Li metal anode in rechargeable batteries.

Keywords: Li-metal batteries, concentrated electrolyte, LiODFB, high temperature, dendrites free

OPEN ACCESS

Edited by:

Junchao Zheng,
Central South University, China

Reviewed by:

Haisheng Fang,
Kunming University of Science and
Technology, China

Chaoyi Chen,
Guizhou University, China

Ying Hong Yang,
Northeastern University, China

*Correspondence:

Zhao Fang
fangzhao@xauat.edu.cn

Specialty section:

This article was submitted to
Electrochemistry,
a section of the journal
Frontiers in Chemistry

Received: 21 April 2019

Accepted: 26 June 2019

Published: 18 July 2019

Citation:

Yu J, Gao N, Peng J, Ma N, Liu X,
Shen C, Xie K and Fang Z (2019)
Concentrated LiODFB Electrolyte for
Lithium Metal Batteries.
Front. Chem. 7:494.
doi: 10.3389/fchem.2019.00494

INTRODUCTION

In the past several decades, Li-ion batteries have played successful role in the consumable electronic device market (Etacheri et al., 2011; Goodenough and Kim, 2014). However, the limited specific capacity of the graphite anode limits its wider applications. The theoretical capacity of graphite is only 372 mAh g⁻¹, so it is difficult to achieve the urgent need for high-energy density batteries to adapt to the electrical miniaturization trend (Placke et al., 2017). Based on this reason, the Li metal batteries (LMBs) have attracted wide attention because of its high theoretical specific capacity of 3,860 mAh g⁻¹, small density of 0.534 g cm⁻³ and the relatively negative electrochemical potential (-3.040 V vs. Li/Li⁺) (Zhamu et al., 2012). However, the shortcomings of LMBs are also a headache, such as unsatisfied Coulombic efficiency (CE) and dendritic Li growth. In addition, poor cycle performance caused by Li dendrites seriously affected the commercial development of LMBs.

Significant efforts have been made in the past to solve these problems, including prepare the current collector (Yang et al., 2015; Liang et al., 2016; Zhang et al., 2016; Shi et al., 2017), *ex-situ* protective coating of Li anode (Thompson et al., 2011; Kozen et al., 2015), introduce the battery intermediate protective layer (Liang et al., 2015; Wu et al., 2015; Cheng et al., 2016; Xie et al., 2016, 2017), and electrolyte modification. Electrolyte, which occupies 15% of the weight and about 32% of the volume of the entire battery, is a key part of a battery (Cekic-Laskovic et al., 2017). Therefore, the study of electrolyte on the development of Li metal secondary battery is of great significance. Meanwhile, compared to other modification methods, electrolyte modification is more convenient and cost-effective. Till now, electrolyte research progress more or less has been made to

address the dendrite problem. Nevertheless, the compatibility of these electrolytes with cathode has usually been overlooked. For example, some film-forming electrolyte additives, such as vinylene carbonate (VC) and fluoroethylene carbonate (FEC) are helpful to change Li dendrite formation nature (Aurbach et al., 2003; Jung et al., 2013; Webb et al., 2014; Qian et al., 2016; Pritzl et al., 2017; Xu et al., 2017), but the cell's internal resistance is greatly increased, particularly after long-term cycling, and thus limits their wide applications.

Recently, the concept of high concentrated electrolyte gets into the eyes of people. Suo et al. reported a new class of non-aqueous liquid "Solvent-in-Salt" electrolytes and applied them in Li-S batteries. It is demonstrated that the use of "Solvent-in-Salt" electrolyte inhibits the dissolution of polysulphide and protects metallic Li anodes against the formation of Li dendrites, effectively (Suo et al., 2013). A significant breakthrough has been achieved by Qian et al. (2015). They found that, with 4 M lithium bis(fluorosulfonyl)imide (LiFSI) in DME as the electrolyte, a Li/Li cell can be cycled for more than 6,000 cycles. Meanwhile, a Cu/Li cell can be cycled for more than 1,000 cycles with an average CE of 98.4%, without dendrite growth. Nevertheless, the compatibility of the electrolyte with the cathode materials has not been investigated.

Generally, LiFSI has inherent characteristics of corrosion of aluminum (Al) foil and other metal parts in the battery (Abouimrane et al., 2009; Li et al., 2011). To solve this problem, Park et al. found that lithium borate salts are the ideal additives as corrosion inhibitors in LiFSI electrolytes. The inhibition ability of Al is revealed to be in the following order: lithium oxalyldifluoroborate (LiODFB) > lithium tetrafluoroborate (LiBF_4) > lithium hexafluorophosphate (LiPF_6) > lithium bis(oxalato)borate (LiBOB) (Park et al., 2015). Noticed that LiODFB is considered to combine the half structures of LiBOB and LiBF_4 , and thus, it combines the advantages of LiBOB and LiBF_4 (Zhang, 2006). The main advantages of this salt is given by low viscosity, high ionic conductivity, good film-forming, high temperature performance, good compatibility with the positive electrode, passivation of Li foil and so on (Liu et al., 2007; Zugmann et al., 2011; Wu et al., 2012; Zhou et al., 2012).

However, it should be noted that previous studies (Zhang et al., 2010; Li et al., 2015; Zhou et al., 2016; Bian et al., 2017) only focused on the effect of LiODFB as an additive or auxiliary salt on battery performances. So far, high concentration of LiODFB single salt in ether solvent for LMBs has not been systematically reported before (Zhang et al., 2015; Poyraz et al., 2019; Yamada et al., 2019). Thus, in this work, we first employed the concentrated electrolyte based on LiODFB in LMBs. Due to its increased availability of Li^+ concentration, a highly uniform and stable solid electrolyte interface (SEI) film was formed on Li metal anode without any dendrite. Meanwhile, the compatibility of concentrated LiODFB electrolyte and LiFePO_4 cathode was first investigated by the electrochemical performance of Li/ LiFePO_4 cell at room temperature and high temperature. We found that 4 M LiODFB-DME significantly improve electrochemical performance of LiFePO_4 cathode, compared to LiPF_6 electrolyte. In particular, at high temperature, the improvement is much greater. In a sense, our work shows

concentrated LiODFB electrolyte may have great potential for LMBs.

EXPERIMENTAL SECTION

Electrolytes and Electrode Preparation

The LiPF_6 dissolved in ethylene carbonate (EC), ethyl methyl carbonate (EMC), dimethyl carbonate (DMC) with a volume ratio of 1:1:1 was formed 1.0 M LiPF_6 electrolyte and used as the blank electrolyte. LiODFB was purchased from Suzhou Fluolyte Co., Ltd., China. LiODFB was dissolved in dimethyl ether (DME) and formed 4 M LiODFB-DME in an Ar-filled glove box ($\text{H}_2\text{O} < 0.1$ ppm, $\text{O}_2 < 0.1$ ppm). The electrolytes were stirred to maintain homogeneity, then sealed and stored in the glove box.

The LiFePO_4 cathodes were prepared by mixing 80 wt.% LiFePO_4 (Aladdin Co., Ltd. China), 10 wt.% conductive carbon, and 10 wt.% polyvinylidene (PVDF, Solef) binder in N-methylpyrrolidone (Kelong, Chengdu). The mixed slurry was coated onto Al foil and then dried overnight at 110°C under vacuum. Disk-shaped electrodes with a diameter of 13 mm were then punched from the foil (the active material loading was 1.52 mg cm^{-2}). CR2016 coin-type cells were assembled in an Ar-filled glove box with an LiFePO_4 cathode working electrode, a Li foil counter electrode, and a polypropylene (Celgard 2400) separator; 45 mL of electrolyte was then injected into the cells. Finally, the assembled coin cells were sealed for further tests. Li/Li and Li/Cu cells with different electrolyte solutions and the above-mentioned separator were assembled for further tests.

Electrochemical Measurements

The assembled Li/ LiFePO_4 coin cells were left to stand for 10 h before galvanostatic precycling for 200 cycles at 1°C ($1^\circ\text{C} = 170 \text{ mAh g}^{-1}$) between 2.5 and 4.2 V at 25°C using the Land battery test system (Wuhan LANHE Electronics, China). Rate-performance tests were conducted by changing the rate (0.2, 0.5, 1.0, 2.0, 5.0, and 0.2°C) every 10 cycles. Cyclic voltammetry (CV) and electrochemical impedance spectroscopy (EIS) measurements were carried out using a SI-1287 Electrochemical System (Transmission Precision Measurement Company, UK); the CV tests were performed between 2.5 and 4.2 V at a scan rate of 0.1 mV s^{-1} and the EIS tests were performed over 100 kHz to 10 mHz range with an amplitude of 10 mV before and after rate tests. Then the assembled cells were galvanostatic precycled at 65°C .

The current density for the Li metal plating/stripping was set to 1.0 mA cm^{-2} using a Land battery testing station at room temperature. And the deposition time was 1.5 h. The effective area of the Cu foil for Li deposition was 2.11 cm^2 . The current density was 1.0 mA cm^{-2} from 0.01 to 1.00 V. Li/Li symmetric cells were assembled with Li metal used as the working and counter electrodes. The batteries were tested in a Tenney JR environmental chamber to ensure the stable temperature during long-term cycling process.

Morphological Characterizations

Scanning electron microscopy (SEM) (FE-SEM, LEO 1530) was employed to observe the surface topography of the LiFePO_4

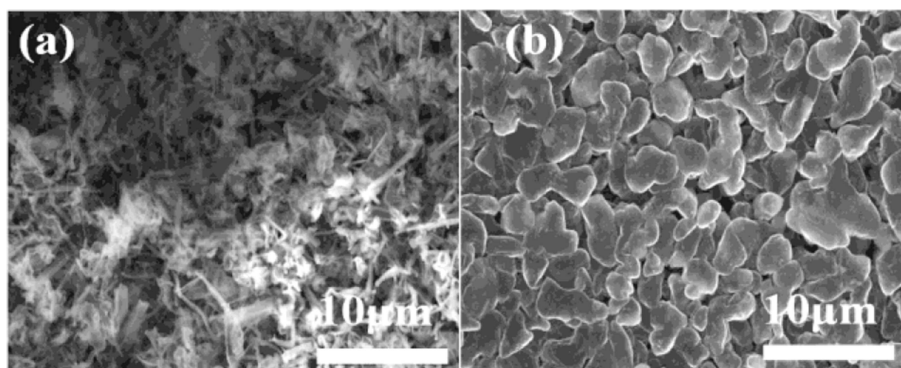


FIGURE 1 | SEM images of the morphologies of Li after plating on Cu substrates in different electrolytes. **(a)** 1 M LiPF₆ electrolyte; **(b)** 4 M LiODFB-DME. The current density was 1.0 mA cm⁻² and the deposition time was 1.5 h.

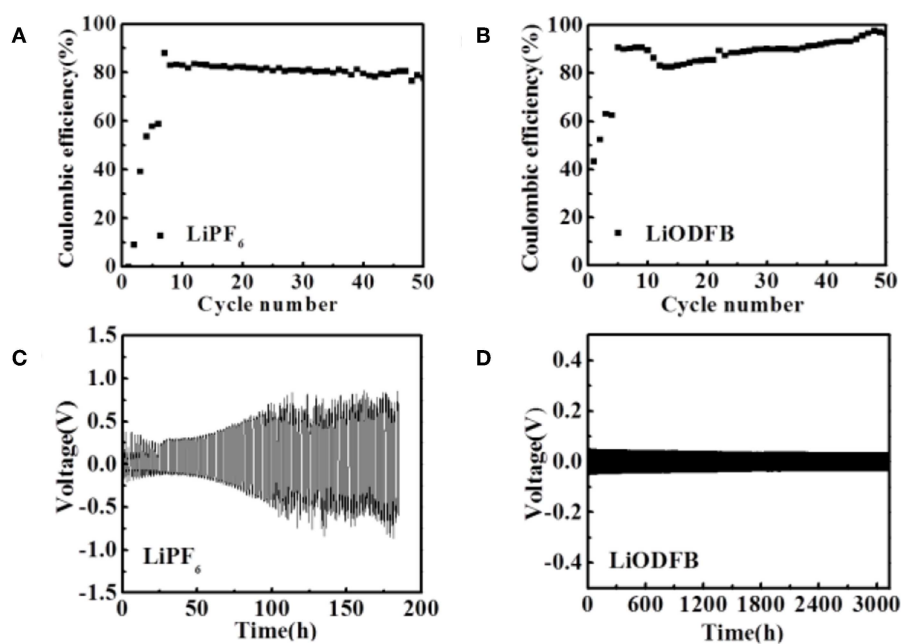


FIGURE 2 | Electrochemical performances of Li/Cu cell **(A,B)** and Li/Li cells **(C,D)** with two electrolytes at a current density of 1.0 mA cm⁻². **(A,C)** the 1 M LiPF₆ electrolyte; **(B,D)** the 4 M LiODFB-DME.

electrode and Cu foil at different cycling stages at an accelerating voltage of 5 kV. The XPS is tested to further study the composition of SEI film on the Cu foil by the Thermo Electron model K-Alpha surface analysis system. The electrodes retrieved from the cells were thoroughly rinsed in high purity dimethyl carbonate (DMC) solvent for three times and dried under vacuum before transferring to the observation chamber.

EXPERIMENTAL RESULTS

Li Metal Deposition Morphology

The morphologies of Li deposition in both electrolytes are evaluated by using coin-type Cu/Li cells. The surface morphologies of Li electrodes cycled after 1.5 h in different

electrolytes is shown in **Figure 1**. In conventional carbonate based electrolyte, significant dendrite morphology can be observed (**Figure 1a**). It can easily pierce most conventional separators, causing the direct contact of the positive and negative electrodes to form a short circuit, and lead to serious security risks. On the contrary, Li deposit from the 4 M LiODFB-DME electrolyte exhibits smooth solid particle morphology (**Figure 1b**), which dramatically inhibits the growth of Li dendrite. Based on the Li metal deposition morphologies, it is reasonable to conclude that the 4 M LiODFB-DME has good negative electrode stability. The SEI film formed in the high concentration electrolyte has high ionic conductivity, which makes a uniform and stable SEI film formed. The uniform and stable SEI film can suppress the growth of Li dendrite.

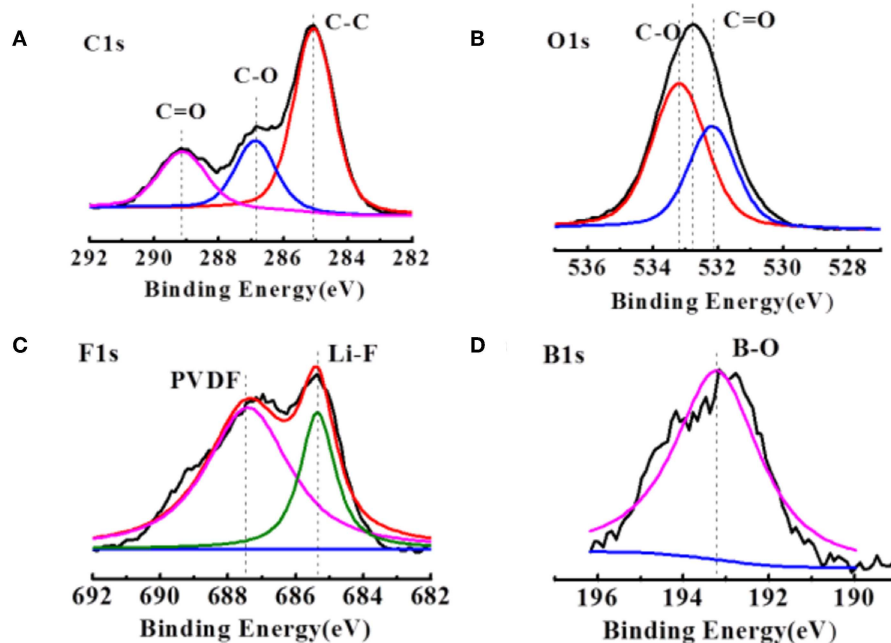


FIGURE 3 | XPS patterns of (A,B) the cycled Li anodes in the LiODFB electrolyte. (C,D) The cycled electrodes were disassembled from the Li/Li cells after 1.5 h.

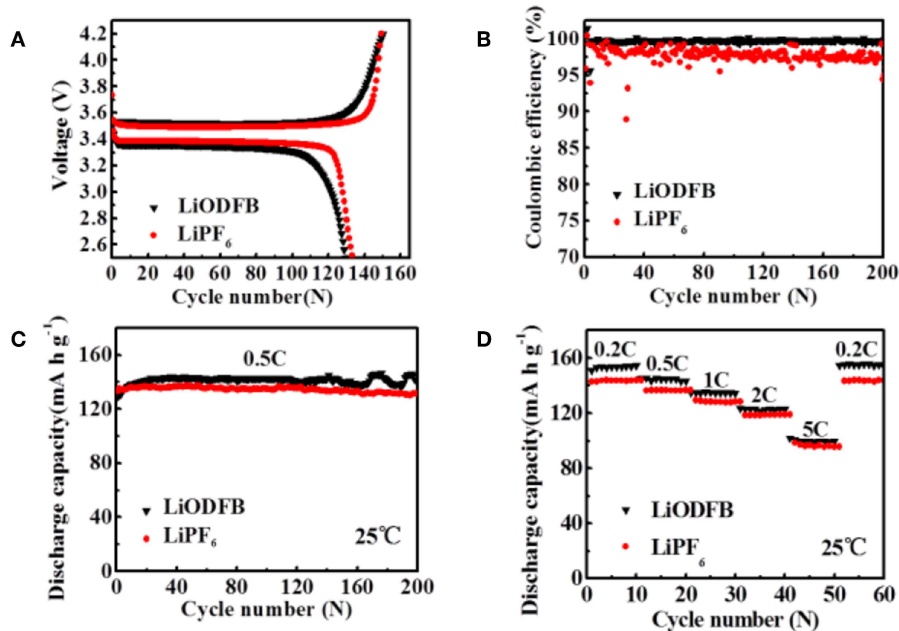


FIGURE 4 | (A) first charge/discharge profiles of the Li/LiFePO₄ cells, (B) CE of Li/LiFePO₄ cells; (C,D) cycle performance of Li/LiFePO₄ cells at 25°C with 4 M LiODFB-DME and 1 M LiPF₆, (D) rate performances of Li/LiFePO₄ cells at 25°C with 4 M LiODFB-DME and 1 M LiPF₆.

Li Metal Plating/Stripping Cycling Stability

The impedance evolution of the coin-type Cu/Li cells after 0.5 h and 1.5 h are depicted in **Figure S1**. In the Nyquist plots, the intercept with the abscissa represents the ohmic resistance, particularly the electrolyte resistance in the cell.

A significant difference in the impedance between the two electrolytes is observed. After 0.5 and 1.5 h of deposition process, the commercial electrolyte exhibits relatively higher electrode impedance **Figure S1A**. At the same time, 4 M LiODFB-DME electrolyte shows small impedance **Figure S1B**.

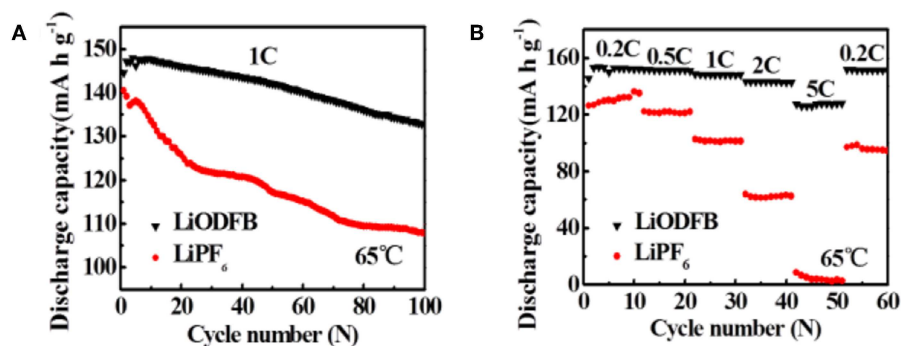


FIGURE 5 | (A) cycle performance of the Li/LiFePO₄ cells at 65°C with 4 M LiODFB-DME and 1 M LiPF₆, **(B)** rate performance of Li/LiFePO₄ cells at 65°C with 4 M LiODFB-DME and 1 M LiPF₆.

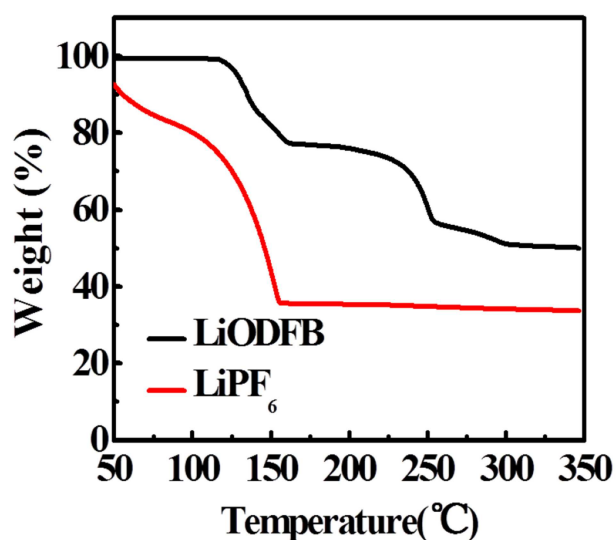


FIGURE 6 | TGA curves of the fully-charged LiFePO₄ electrode cycled in LiODFB and LiPF₆ electrolytes.

The most possible reason for the small impedance is attributed to the formation of the stable SEI film, which is consistent with the results of a dense surface morphology in **Figure 1b**. Polarization measurements of the Li/Li cells were conducted to understand the effect of different electrolytes on stabilizing the interface between the Li metal and electrolyte. During this experiment, a constant deposition/dissolution current density of 1.0 mA cm⁻² was passed through the Li/Li cells for 3,000 h at room temperature. The 1 M LiPF₆ electrolyte shows the great over-voltage and an ascending tendency with time (**Figure 2**), which is consistent with previous report (Webb et al., 2014). Surprisingly, the 4 M LiODFB-DME electrolyte appears excellent Li deposition/dissolution performance with the stable and low over-voltage. Polarization is lower than 1 M LiPF₆ electrolyte. Besides, influenced by high viscosity, on the one hand, it possibly increases the pressure from the electrolyte to push back growing dendrites, resulting in a more uniform deposition on the surface of the anode. On the other hand, high viscosity limits

anion convection near deposition area, which is also helpful to deposit uniformly. All of the above results confirm that the high concentration of LiODFB electrolyte in ether solvent can ensure the cycle stability in the negative.

DISCUSSION

Discussion for the Possible Function Mechanism

Figure 3A compares the C1s spectra of the delithiated graphite electrodes extracted from the cell after several cycles. The dominant peak at 284.6 eV originates mainly from the sp² hybridized graphite, but also includes contributions from conductive carbon added into the electrode composites. The broad feature at 286.6 eV is assigned mainly to the C atoms of the C-O-C groups in the poly(ethylene oxide), PEO, which is formed upon solvent polymerization. The formation of PEO is also confirmed by the peak at 533.6 eV in the O1s XPS spectra in **Figure 3B**. The rather broad peaks at 288.6 eV in **Figure 4A** are assigned to carbon in C=O groups in organic Li alkyl carbonates (ROCO₂Li) and Li carbonates (Li₂CO₃), respectively. The corresponding peak of the oxygen atoms in these groups is detected in the O1s spectra (**Figure 3C**) at 531.8 eV. **Figure 3C**, the F1s peak at 687.5 eV are assigned with PVDF, while the peak at 684.2 eV corresponding to LiF is much stronger, agreeing with the inorganic inner layer of SEI. However, there is almost no difference in contrast to the case of the commercial electrolyte in the C1s, O1s, and F1s spectra. The difference appears at F1s spectra. The B1s peaks at 193.8 eV and 192.6 eV (**Figure 3D**) indicates the presence of LiODFB and material with B-O, respectively. And no such peak in commercial electrolyte.

This result indicates that the B-O bond is involved in the formation of the film, making the SEI film is much denser (Xu et al., 2016). It is consistent with the results of a dense surface morphology in **Figure 1b**.

The Electrochemical Performances of LiFePO₄ Batteries

The assembled Li/LiFePO₄ coin cells are used to compare the cycling and rate stability using 4 M LiODFB-DME electrolyte and 1 M LiPF₆ electrolyte at room temperature in this part.

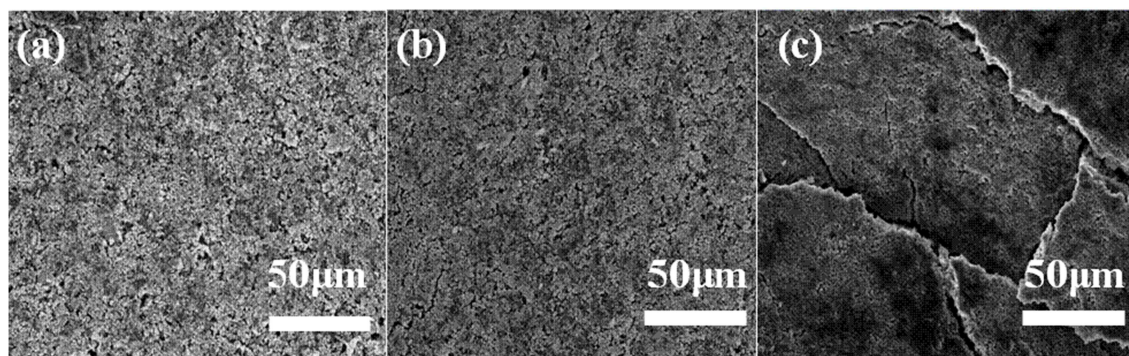


FIGURE 7 | SEM images for pristine cathode **(a)** cathodes after 100 cycles at 65°C with **(b)** the 4 M LiODFB-DME; **(c)** the 1 M LiPF₆.

Figure 4A shows the first charge/discharge profiles of the cells in different electrolytes at the 0.2°C current rate (1°C = 170 mAh g⁻¹). The cells are initially activated at 0.2°C for three cycles and then cycled at 0.5°C. The cells display similar voltage curves, but the cell using the 4 M LiODFB-DME electrolyte exhibits slightly smaller discharge capacities of 129 mAh g⁻¹, while the initial discharge capacity of 1 M LiPF₆ is 133 mAh g⁻¹. The result is directly related to the lower ionic conductivity of 4 M LiODFB-DME electrolyte compared to LiPF₆-based electrolyte. The long-term cycling performances of Li/LiFePO₄ cells are depicted in **Figure 4C**. There is no obvious difference after 200 cycles, and 4 M LiODFB-DME electrolyte shows little superiority compared to commercial LiPF₆-based electrolyte. However, LiODFB electrolyte shows excellent CE of 99% over 200 cycles; while the cell with the LiPF₆ is only 89% after 200 cycles (**Figure 4B**). It shows that LiODFB salt greatly improves the cycling stability, but the delivered capacity might have been hindered by the electrolyte's undesirable ionic conductivity. **Figure 4D** presents the rate capability of Li/LiFePO₄ cell in 1 M LiPF₆ and 4 M LiODFB-DME electrolytes. Discharge capacity of cells with 4 M LiODFB-DME are 154.8 mAh g⁻¹ at 0.2°C, 143.3 mAh g⁻¹ at 0.5°C, 134.4 mAh g⁻¹ at 1.0°C, 123.1 mAh g⁻¹ at 2.0°C, and 99.5 mAh g⁻¹ at 5.0°C. As comparison, discharge capacity of cells with 1 M LiPF₆ are 143.9 mAh g⁻¹ at 0.2°C, 136.7 mAh g⁻¹ at 0.5°C, 128.3 mAh g⁻¹ at 1.0°C, 118.9 mAh g⁻¹ at 2.0°C, and 95.8 mAh g⁻¹ at 5.0°C. Voltage profiles of both cells are also very similar **Figure S2**. It seems that discharged capacity at different cycling rates of cells with 4 M LiODFB-DME electrolyte are slightly higher than cells with 1 M LiPF₆ electrolyte. The outstanding thermal stability and water stability LiODFB leads to very weak side reactions and the dissolution of iron is suppressed. These are the reasons of better cycling performance of cells in 4 M LiODFB-DME electrolyte. All in all, the electrochemical performances of the two electrolytes capacity reach a considerable level at room temperature. These also can be confirmed on the impedance test results in **Figure S2**.

Furthermore, the cycling performances of Li/LiFePO₄ cells at 65°C are assessed in both electrolytes (**Figure 5A**). In **Figure 5A**, when the cell is working in LiPF₆ electrolyte, the capacity decay

rapidly after cycles. We can discover it only has capacity retention of 79.3% after 100 cycles, which is consistent with the result reported by ZHANG et al. As a comparison, excellent cycle stability is observed when using 4 M LiODFB-DME electrolyte, with high capacity retention of 92.5% after 100 cycles. The rate capability of Li/LiFePO₄ at 65°C in different electrolytes is obtained in **Figure 5B**. Much larger discharge capacities are showed at higher rates for the 4 M LiODFB-DME. For example, the LiPF₆ electrolyte shows discharge capacities of 101.1 and 62.5 mAh g⁻¹ at the 1.0 and 2.0°C rates, respectively, even the capacities of cell is almost close to zero at 5.0°C; While these values are increased to 148.1, 142.8, 127.7 mAh g⁻¹ at the 1.0, 2.0, and 5.0°C rates for the LiODFB electrolyte. This demonstrates that LiODFB not only improve the cycling stability but also improve the rate capability in high temperature. It seems that the better thermal stability of LiODFB salts plays an important role in improving the high-temperature resilience of LiFePO₄ electrode.

We used TGA to study the thermal stability of fully charged electrodes in electrolytes (**Figure 6**). Evaporation of the adsorbed organic solvent appears as their weight loss before 150°C in 4 M LiODFB-DME electrolyte. As the heating progressed, a significant weight loss begins to appear at about 250°C, which originates from the decomposition of the SEI film. In contrast, the large-scale weight decay starts at 50°C in 1 M LiPF₆, and the mass attenuation has reached a minimum at 150°C, proving that the SEI film has completely broken before 150°C. It shows that 4 M LiODFB-DME electrolyte produces a more stable SEI film and establishes a more gentle interface between the electrode and the electrolyte. So the fully delithiated electrode is protected from directly contacting with the electrolyte. Therefore, the LiODFB electrolyte improves the thermal stability of the highly oxidized charged electrode.

SEM Micrographs of LiFePO₄ Electrodes

SEM analysis is performed to illustrate electrode images before and after 100 cycles in both electrolytes at 65°C. The LiFePO₄ electrode after long-term cycling in 4 M LiODFB-DME electrolyte (**Figure 7b**) shows a similar morphology to the pristine LiFePO₄ electrode (**Figure 7a**). In comparison, the electrode is severely eroded in 1 M LiPF₆ electrolyte after

100 cycles at 65°C in **Figure 7c**, and we can find that the LiFePO₄ electrode surface in 1 M LiPF₆ electrolyte displays some cracks among the particles. It is result from the poor thermal stability of the 1 M LiPF₆ electrolyte. The decomposition of LiPF₆ in high temperature causes serious capacity decay rapidly, resulting in very poor electrochemical performance, as shown in **Figure 5A**. The higher the current density, this effect is more serious in **Figure 5B**. These SEM observations confirm that 4 M LiODFB-DME electrolyte has excellent compatibility with LiFePO₄ cathodes during battery cycling at high temperature **Figure S3** shows the EDS layered image of LiFePO₄ electrode after 100 cycles at high magnification. The surface of the LiFePO₄ electrode consists of five main elements: O, P, F, and Fe. The Fe and P elements are mainly derived from LiFePO₄ electrode and the O, F, and B elements are derived from LiODFB lithium salt. It is proved that the B element from the LiODFB-based electrolyte participates the formation of the surface film of LiFePO₄ cathode. And the participation of the B elements makes the surface film of LiFePO₄ cathode smooth and compact. All in all, the LiODFB lithium salt protects the cathode. In addition, the SEM images of the morphologies of Al foils is shown in **Figure S4**. The surface of the Al foils had a large difference. The concentrated electrolytes suppress the Al corrosion more effectively.

CONCLUSIONS

In this work, we first developed a concentrated electrolyte based on LiODFB in ether solvents for LMBs. Based on 4 M LiODFB-DME electrolyte, Li was deposited on the copper foil and its surface showed smooth solid particle morphology without any dendrites. For the Li/LiFePO₄ cells, it is demonstrated that 4 M LiODFB-DME electrolyte exhibit good electrochemical performance, especially at the elevated temperature. Li/LiFePO₄

cells using 4 M LiODFB-DME electrolyte show a good capacity retention (92.5%) at elevated temperature (65°C), which is much higher than that of 1 M LiPF₆ electrolyte (79.2%). This research offers the possibility of rapid industrialization of LMBs.

DATA AVAILABILITY

The raw data supporting the conclusions of this manuscript will be made available by the authors, without undue reservation, to any qualified researcher.

AUTHOR CONTRIBUTIONS

ZF and JY conceived and designed the experiments. NG, JP, XL, and NM performed the experiments. NG, CS, and XL analyzed the data. NG and NM wrote the manuscript. KX designed the scheme. All authors reviewed the manuscript and approved the final version.

ACKNOWLEDGMENTS

We acknowledge the financial support of this work by the Project (51574191, 51304151) supported by the National Natural Science Foundation of China; Project (18JK0474) supported by Shaanxi Provincial Education Department, China; Project (2018JM5135) supported by the Natural Science Basic Research Plan in Shaanxi Province, China.

SUPPLEMENTARY MATERIAL

The Supplementary Material for this article can be found online at: <https://www.frontiersin.org/articles/10.3389/fchem.2019.00494/full#supplementary-material>

REFERENCES

- Abouimrane, A., Ding, J., and Davidson, I. J. (2009). Liquid electrolyte based on lithium bis-fluorosulfonyl imide salt: Al corrosion studies and lithium ion battery investigations. *J. Power Sources* 189, 693–696. doi: 10.1016/j.jpowsour.2008.08.077
- Aurbach, D., Gamolsky, K., Markovsky, B., Gofer, Y., Schmidt, M., Heider, U., et al. (2003). On the use of vinylene carbonate (VC) as an additive to electrolyte solutions for Li-ion batteries. *Electrochim. Acta* 47, 1423–1439. doi: 10.1016/S0013-4686(01)00858-1
- Bian, X., Ge, S., Pang, Q., Zhu, K., Wei, Y., Zou, B., et al. (2017). A novel lithium difluoro(oxalate) borate and lithium hexafluoride phosphate dual-salt electrolyte for Li-excess layered cathode material. *J. Alloy. Compd.* 736, 136–142. doi: 10.1016/j.jallcom.2017.11.126
- Cekic-Laskovic, I., von Aspern, N., Imholt, L., Kaymaksiz, S., Oldiges, K., Rad, B. R., et al. (2017). Synergistic effect of blended components in nonaqueous electrolytes for lithium ion batteries. *Top. Curr. Chem.* 375, 37–100. doi: 10.1007/s41061-017-0125-8
- Cheng, X. B., Hou, T. Z., Zhang, R., Peng, H. J., Zhao, C. Z., Huang, J. Q., et al. (2016). Dendrite-free lithium deposition induced by uniformly distributed lithium ions for efficient lithium metal batteries. *Adv. Mater.* 28, 2888–2895. doi: 10.1002/adma.201506124
- Etacheri, V., Marom, R., Elazari, R., Salitra, G., and Aurbach, D. (2011). Challenges in the development of advanced Li-ion batteries: a review. *Energy Environ. Sci.* 4, 3243–3262. doi: 10.1039/C1EE01598B
- Goodenough, J. B., and Kim, Y. (2014). Challenges for rechargeable li batteries. *Chem. Mater.* 22, 587–603. doi: 10.1021/cm901452z
- Jung, H., Park, S. H., Jeon, J., Choi, Y., Yoon, S., Cho, J. J., et al. (2013). Fluoropropane sultone as an SEI-forming additive that outperforms vinylene carbonate. *J. Mater. Chem.* 1, 11975–11981. doi: 10.1039/C3TA12580G
- Kozen, A. C., Lin, C. F., Pearse, A. J., Schroeder, M. A., Han, X., Hu, L., et al. (2015). Next-generation lithium metal anode engineering via atomic layer deposition. *ACS Nano* 9, 5884–5892. doi: 10.1021/acsnano.5b02166
- Li, F., Gong, Y., Jia, G., Wang, Q., Peng, Z., Fan, W., et al. (2015). A novel dual-salts of LiTFSI and LiODFB in LiFePO₄-based batteries for suppressing Al corrosion and improving cycling stability. *J. Power Sources* 295, 47–54. doi: 10.1016/j.jpowsour.2015.06.117
- Li, L., Zhou, S., Han, H., Li, H., Nie, J., Armand, M., et al. (2011). Transport and electrochemical properties and spectral features of non-aqueous electrolytes containing LiFSI in linear carbonate solvents. *J. Electrochem. Soc.* A 158, 74–82. doi: 10.1149/2.jes120006
- Liang, Z., Lin, D., Zhao, J., Lu, Z., Liu, Y., Liu, C., et al. (2016). Composite lithium metal anode by melt infusion of lithium into a 3D conducting scaffold with lithiophilic coating. *Proc. Natl. Acad. Sci. U.S.A.* 113, 2862–2867. doi: 10.1073/pnas.1518188113

- Liang, Z., Zheng, G., Liu, C., Liu, N., Li, W., Yan, K., et al. (2015). Polymer nanofiber-guided uniform lithium deposition for battery electrodes. *Nano Lett.* 15, 2910–2916. doi: 10.1021/nl5046318
- Liu, J., Chen, Z., Busking, S., and Amine, K. (2007). Lithium difluoro(oxalato)borate as a functional additive for lithium-ion batteries. *Electrochem. Commun.* 9, 475–479. doi: 10.1016/j.elecom.2006.10.022
- Park, K., Yu, S., Lee, C., and Lee, H. (2015). Comparative study on lithium borates as corrosion inhibitors of Al current collector in lithium bis(fluorosulfonyl)imide electrolytes. *J. Power Sources* 296, 197–203. doi: 10.1016/j.jpowsour.2015.07.052
- Placke, T., Kloepsch, R., Dühnen, S., and Winter, M. (2017). Lithium ion, lithium metal, and alternative rechargeable battery technologies: the odyssey for high energy density. *J. Solid State Electrochem.* 21, 1939–1964. doi: 10.1007/s10008-017-3610-7
- Poyraz, A. S., Laughlin, J., and Zec, Z. (2019). Improving the cycle life of cryptomelane type manganese dioxides in aqueous rechargeable zinc ion batteries: the effect of electrolyte concentration. *Electrochim. Acta* 305, 423–432. doi: 10.1016/j.electacta.2019.03.093
- Pritzl, D., Solchenbach, S., Wetjen, M., and Gasteiger, H. A. (2017). Analysis of vinylene carbonate (VC) as additive in graphite/LiNi_{0.5}Mn_{1.5}O₄ cells. *J. Electrochem. Soc. A* 164, 2625–2635. doi: 10.1149/2.1441712jes
- Qian, J., Henderson, W. A., Xu, W., Bhattacharya, P., Engelhard, M., Borodin, O., et al. (2015). High rate and stable cycling of lithium metal anode. *Nat. Commun.* 6, 6362–6370. doi: 10.1038/ncomms7362
- Qian, Y., Schultz, C., Niehoff, P., Schwieters, T., Nowak, S., Winter, M., et al. (2016). Investigations on the electrochemical decomposition of the electrolyte additive vinylene carbonate in Li metal half cells and lithium ion full cells. *J. Power Sources* 332, 60–71. doi: 10.1016/j.jpowsour.2016.09.100
- Shi, L., Xu, A., and Zhao, T. (2017). First-principles investigations of the working mechanism of 2D h-BN as an interfacial layer for the anode of lithium metal batteries. *ACS Appl. Mater. Inter.* 9, 1987–1994. doi: 10.1021/acsami.6b14560
- Suo, L., Hu, Y. S., Li, H., Armand, M., and Chen, L. (2013). A new class of Solvent-in-Salt electrolyte for high-energy rechargeable metallic lithium batteries. *Nat. Commun.* 4, 1481–1489. doi: 10.1038/ncomms2513
- Thompson, R. S., Schroeder, D. J., Lopez, C. M., Neuhold, S., and Vaughey, J. T. (2011). Stabilization of lithium metal anodes using silane-based coatings. *Electrochem. Commun.* 13, 1369–1372. doi: 10.1016/j.elecom.2011.08.012
- Webb, S. A., Baggetto, L., Bridges, C. A., and Veith, G. M. (2014). The electrochemical reactions of pure indium with Li and Na: anomalous electrolyte decomposition, benefits of FEC additive, phase transitions and electrode performance. *J. Power Sources* 248, 1105–1117. doi: 10.1016/j.jpowsour.2013.10.033
- Wu, F., Ye, Y., Chen, R., Qian, J., Zhao, T., Li, L., et al. (2015). A systematic effect for an ultra-long cycle lithium-sulfur battery. *Nano Lett.* 15, 7431–7439. doi: 10.1021/acs.nanolett.5b02864
- Wu, Q., Lu, W., Miranda, M., Honaker-Schroeder, T. K., Lakhsassi, K. Y., Dees, D., et al. (2012). Effects of lithium difluoro(oxalate)borate on the performance of Li-rich composite cathode in Li-ion battery. *Electrochem. Commun.* 24, 78–81. doi: 10.1016/j.elecom.2012.08.016
- Xie, K., Wei, W., Yuan, K., Lu, W., Guo, M., Li, Z., et al. (2016). Toward dendrite-free lithium deposition via structural and interfacial synergistic effects of 3D graphene@Ni scaffold. *ACS Appl. Mater. Interfaces* 8, 26091–26097. doi: 10.1021/acsami.6b09031
- Xie, K., Yuan, K., Zhang, K., Shen, C., Lv, W., Liu, X., et al. (2017). Dual functionalities of carbon nanotube films for dendrite-free and high energy-high power lithium-sulfur batteries. *ACS Appl. Mater. Interfaces* 9, 4605–4613. doi: 10.1021/acsami.6b14039
- Xu, Y., Liu, J., Zhou, L., Zeng, L., and Yang, Z. (2017). FEC as the additive of 5 V electrolyte and its electrochemical performance for LiNi_{0.5}Mn_{1.5}O₄. *J. Electroanal. Chem.* 791, 109–116. doi: 10.1016/j.jelechem.2017.03.017
- Xu, Z., Wang, J., Yang, J., Miao, X., Chen, R., Qian, J., et al. (2016). Enhanced performance of a lithium-sulfur battery using a carbonate-based electrolyte. *Angew. Chem. Int. Ed.* 55, 10372–10375. doi: 10.1002/anie.201605931
- Yamada, Y., Wang, J., Ko, S., Watanabe, E., and Yamada, A. (2019). Advances and issues in developing salt-concentrated battery electrolytes. *Nat. Nanotechnol.* 14, 200–207. doi: 10.1038/s41560-019-0336-z
- Yang, C. P., Yin, Y. X., Zhang, S. F., Li, N. W., and Guo, Y. G. (2015). Accommodating lithium into 3D current collectors with a submicron skeleton towards long-life lithium metal anodes. *Nat. Commun.* 6, 8058. doi: 10.1038/ncomms9058
- Zhamu, A., Chen, G., Liu, C. G., Neff, D., Fang, Q., Yu, Z. N., et al. (2012). Reviving rechargeable lithium metal batteries: enabling next-generation high-energy and high-power cells. *Energy Environ. Sci.* 5, 5701–5707. doi: 10.1039/C2EE02911A
- Zhang, R., Cheng, X. B., Zhao, C. Z., Peng, H. J., Shi, J. L., Huang, J. Q., et al. (2016). Conductive nanostructured scaffolds render low local current density to inhibit lithium dendrite growth. *Adv. Mater.* 28, 2155–2162. doi: 10.1002/adma.201504117
- Zhang, S. S. (2006). An unique lithium salt for the improved electrolyte of Li-ion battery. *Electrochem. Commun.* 9, 1423–1428. doi: 10.1016/j.elecom.2006.06.016
- Zhang, Z., Chen, X., Li, F., Lai, Y., Li, J., Liu, P., et al. (2010). LiPF₆ and lithium oxalyldifluoroborate blend salts electrolyte for LiFePO₄/artificial graphite lithium-ion cells. *J. Power Sources* 21, 7397–7402. doi: 10.1016/j.jpowsour.2010.05.056
- Zhang, Z. A., Zhao, X. X., Peng, B., Lai, Y. Q., Zhang, Z. Y., Li, J., et al. (2015). Mixed salts for lithium iron phosphate-based batteries operated at wide temperature range. *Transac. Nonferr. Metal. Soc.* 25, 2260–2265. doi: 10.1016/S1003-6326(15)63839-0
- Zhou, H., Liu, F., and Li, J. (2012). Preparation, thermal stability and electrochemical properties of LiODFB. *J. Mater. Sci. Technol.* 28, 723–727. doi: 10.1016/S1005-0302(12)60121-2
- Zhou, H., Xiao, K., and Li, J. (2016). Lithium difluoro(oxalate)borate and LiBF₄ blend salts electrolyte for LiNi_{0.5}Mn_{1.5}O₄ cathode material. *J. Power Sources* 302, 274–282. doi: 10.1016/j.jpowsour.2015.10.073
- Zugmann, S., Moosbauer, D., Amereller, M., Schreiner, C., and Wudy, F. (2011). Electrochemical characterization of electrolytes for lithium-ion batteries based on lithium difluoromono(oxalato)borate. *J. Power Sources* 196, 1417–1424. doi: 10.1016/j.jpowsour.2010.08.023

Conflict of Interest Statement: The authors declare that the research was conducted in the absence of any commercial or financial relationships that could be construed as a potential conflict of interest.

Copyright © 2019 Yu, Gao, Peng, Ma, Liu, Shen, Xie and Fang. This is an open-access article distributed under the terms of the Creative Commons Attribution License (CC BY). The use, distribution or reproduction in other forums is permitted, provided the original author(s) and the copyright owner(s) are credited and that the original publication in this journal is cited, in accordance with accepted academic practice. No use, distribution or reproduction is permitted which does not comply with these terms.